

The mechanical power output of the pectoralis muscle of blue-breasted quail (*Coturnix chinensis*): the *in vivo* length cycle and its implications for muscle performance

Graham N. Askew^{1,*} and Richard L. Marsh²

¹Department of Zoology, Downing Street, University of Cambridge, Cambridge CB2 3EJ, UK and

²Department of Biology, Northeastern University, 360 Huntington Avenue, Boston, MA 02115, USA

*Author for correspondence at present address: School of Biology, University of Leeds, Leeds LS2 9JT, UK (e-mail: g.n.askew@leeds.ac.uk)

Accepted 27 July 2001

Summary

Sonomicrometry and electromyographic (EMG) recordings were made for the pectoralis muscle of blue-breasted quail (*Coturnix chinensis*) during take-off and horizontal flight. In both modes of flight, the pectoralis strain trajectory was asymmetrical, with 70% of the total cycle time spent shortening. EMG activity was found to start just before mid-upstroke and continued into the downstroke. The wingbeat frequency was 23 Hz, and the total strain was 23% of the mean resting length.

Bundles of fibres were dissected from the pectoralis and subjected *in vitro* to the *in vivo* length and activity patterns, whilst measuring force. The net power output was only 80 W kg⁻¹ because of a large artefact in the force record during lengthening. For more realistic estimates of the pectoralis power output, we ignored the power absorbed by the muscle bundles during lengthening. The net power output during shortening averaged over the entire cycle was approximately 350 W kg⁻¹, and in several preparations over 400 W kg⁻¹. Sawtooth cycles were also

examined for comparison with the simulation cycles, which were identical in all respects apart from the velocity profile. The power output during these cycles was found to be 14% lower than during the *in vivo* strain trajectory. This difference was due to a higher velocity of stretch, which resulted in greater activation and higher power output throughout the later part of shortening, and the increase in shortening velocity towards the end of shortening, which facilitated deactivation.

The muscle was found to operate at a mean length shorter than the plateau of the length/force relationship, which resulted in the isometric stress measured at the mean resting length being lower than is typically reported for striated muscle.

Key words: blue-breasted quail, *Coturnix chinensis*, muscle mechanics, power output, sonomicrometry, electromyography, work loop, strain trajectory.

Introduction

The mechanical performance of a skeletal muscle during movement is determined by the interaction between its physiological properties and the load upon which it acts (Marsh, 1999). For muscles that produce power in repetitive contractions, the magnitude of the power output is a function of the strain (or velocity) trajectory and the phase and duration of stimulation with respect to this trajectory (Askew and Marsh, 1997; Askew and Marsh, 1998; Girgenrath and Marsh, 1999). The strain trajectory is determined by the nature of the load and how this load responds as the muscle acts on it. The central premise of the work presented here is that the details of the strain trajectory are critical for performance, and we must examine these details if we are to understand how natural selection has acted on the physiology and morphology of animals to shape performance.

During cyclical contractions, muscular power is only contributed during the shortening phase of the cycle, whilst

work is required to re-lengthen the muscle. During activities in which there are distinct power-generating and recovery strokes, and that also require a high power output, some animals prolong the phase of the cycle during which the muscle shortens (i.e. the power-generating stage). For example, during jet propulsion swimming in the scallop *Chlamys hastata*, the adductor muscle shortens for up to 65% of the contraction cycle (Marsh et al., 1992). The external oblique muscles of the tree frog *Hyla versicolor* undergo length changes during vocalisation in which as much as 75% of the time is spent shortening (Girgenrath and Marsh, 1997). Similarly, during flight, the main power stroke (the downstroke) is sometimes longer than the upstroke [e.g. 63% in pigeons (Biewener et al., 1998); 60% in hawkmoths *Manduca sexta* (Willmott and Ellington, 1997)], particularly during take-off [e.g. 63% in osprey (G. Askew, personal observation); 70% in Rüpell's griffon vulture (Scholey, 1983)]. In some fish that use

primarily their pectoral fins to generate thrust, the propulsive downstroke lasts for approximately 70% of the total beat duration (Westneat, 1996).

Askew and Marsh (Askew and Marsh, 1997) investigated the effects of such asymmetrical cycles on the net power output of mouse skeletal muscles *in vitro*, using the work loop technique, and found that the net power output increased as the proportion of the time spent shortening increased. The enhancement of net power was attributable to more complete activation of the muscle, an increase in the optimal strain amplitude and a decrease in the time required to activate the muscle. Manipulation of the strain trajectory allowed the net power output during cyclical contractions to reach 70% of the peak isotonic power output determined for the force/velocity curve.

Other *in vitro* work suggests that altering the rate of lengthening and shortening may further improve power output by changing the rate of activation and deactivation. On the basis of the force/velocity relationship, some investigators have suggested that muscles should operate at a constant shortening velocity to maximize the net power output during cyclical contractions. For a particular muscle, this shortening velocity is dependent on the maximum velocity of shortening and the curvature of the force/velocity relationship. Typically, the optimum relative shortening velocity (V/V_{\max}) for maximizing power output on the basis of the force/velocity relationship is 0.2–0.4 [e.g. Rome (Rome, 1994)]. However, Askew and Marsh (Askew and Marsh, 1998) showed that the optimal V/V_{\max} for mouse soleus muscle performing cyclical contractions depended on the cycle frequency and the strain trajectory. Under conditions in which the strain amplitude was high (i.e. low cycle frequencies and cycles in which the proportion of the cycle spent shortening was greater than that spent lengthening), the optimum V/V_{\max} was lower than that predicted from the force/velocity relationship because of the effects of the length/force relationship. At high cycle frequencies and during strain trajectories in which the proportion of the cycle spent shortening was shorter than that spent lengthening, the optimal V/V_{\max} was higher than that predicted from the force/velocity relationship. The reasons were complex, but were related to the time required to activate and deactivate the muscle. The rate of activation increased with increasing lengthening velocity, and the rate of deactivation increased with increasing shortening velocity. These effects were termed velocity-dependent activation and deactivation, respectively (Askew and Marsh, 1998). We hypothesized that animals might be able to take advantage of these effects to enhance power output by altering the strain trajectory at appropriate times in the cycle.

In examining the influence of strain trajectory on muscle power output, it is advantageous to examine systems in which power output has been of obvious selective advantage. One such system would appear to be the flight muscles of birds. Forward flapping flight conveys an enormous evolutionary advantage to those animals able to exploit it. However, in powerful flyers, this locomotor mode demands a very high net

power output and requires a higher rate of energy consumption than for other mode of locomotion (Norberg, 1990). The power is required to oscillate the wings to generate the lift required for weight support and to provide thrust to overcome drag. In birds, lift is generated mainly during the downstroke, which is powered by the contraction of the pectoralis muscle. This muscle has its origin at the sternum and inserts on the deltopectoral crest of the humerus (Dial et al., 1991). In some bird species, particularly those with a rapid take-off such as grouse and partridges (order Galliformes), the pectoralis makes up as much as 15–26% of the body mass (Magnan, 1922; Hartman, 1961; Tobalske and Dial, 2000). The upstroke (powered by the supracoracoideus muscle) may also generate useful aerodynamic forces; however, in order to generate a net forward thrust, the forces must be smaller than in the downstroke (Rayner, 1993).

The pectoralis muscle performs work cyclically during flight. In pigeons *Columba livia*, starlings *Sturnus vulgaris* and magpies *Pica pica*, electromyographic (EMG) activity of the pectoralis can be detected at approximately mid-upstroke (Dial et al., 1988; Biewener et al., 1992; Dial et al., 1997; Biewener et al., 1998). This activation phase results in the rapid development of force towards the end of the upstroke (Biewener et al., 1992; Dial and Biewener, 1993; Dial et al., 1997; Biewener et al., 1998). EMG activity and force generation continue into the downstroke and are used to accelerate the wing at the start of the stroke and produce aerodynamic forces throughout the stroke. *In vivo* measurements indicate that force generation is maintained throughout shortening but declines to close to zero by the start of the upstroke (Biewener et al., 1998).

Quail (family Phasianidae) are largely ground-dwelling birds that use brief bursts of flight as a means of escaping predation, although it should be noted that some species of quail do migrate, e.g. *Coturnix coturnix*. Quail typically have wings with a low aspect ratio [(wing span)²/wing area], presumably to allow take-off from dense vegetation, which results in a low aerodynamic efficiency, a high induced power output and a high wingbeat frequency. We hypothesized that, during take-off, the pectoralis would exhibit an asymmetrical strain trajectory in order to generate a sufficiently high net power output and that the details of the shape of the strain cycle would also further enhance power.

To test this hypothesis, we measured muscle strain directly (using sonomicrometry). In addition, we made EMG recordings to determine muscle activity. The combined strain and activity patterns recorded *in vivo* were used to simulate *in vitro* the mechanical performance of the pectoralis. We used the work loop technique to measure force during the cycles and, hence, calculated the net power output. The power output determined *in vitro* was compared with that calculated to be required from the kinematics in the following paper (Askew et al., 2001). Blue-breasted quail (*Coturnix chinensis*) were selected for the experiments because of their small size (approximately 40–50 g) and hence suitability for providing muscle preparations for the *in vitro* experiments. They also

readily performed explosive take-off flights that could easily be accommodated in the laboratory.

Materials and methods

Animals

Blue-breasted quail (*Coturnix chinensis*) were hatched from eggs purchased through Carolina Biological Supply. The chicks were maintained in a brooder for 3 weeks post-hatching and then transferred to a temperature-controlled room at 24 °C with a 12 h:12 h (lights on 06:00–18:00 h) light:dark cycle. They had free access to food (alfalfa sprouts and game bird chow) and water. Experiments were carried out once the birds reached 9 weeks old.

The mean body mass (M_b) of the birds used in this study was 45.7 ± 1.4 g (mean \pm S.E.M., $N=10$).

Pre-surgery: sonomicrometry holders and EMG electrodes

Sonomicrometry was used to determine the length changes performed by the pectoralis using the Sonometrics Digital Ultrasonic Measurement System (Sonometrics Corporation, London, Canada). The process uses a pair of piezoelectric crystals, which generate waves of sound that travel at known velocities through tissue. Distance is calculated from the time taken for the sound to travel between the transmitter and corresponding receiver crystal. The crystals in the Sonometrics system automatically alternate between transmitter and receiver modes, providing two sets of data for each pair of crystals. This system also provides enhanced time resolution compared with older analogue sonomicrometers. In our experiments, we obtained approximately 1000 instantaneous length measurements per second.

To hold the sonomicrometry crystals in place in the muscle, they were attached to holders sutured to the surface of the muscle. The holders were constructed by bending a 000 insect pin into three arms (two arms approximately 1.5 mm long and the other 2 mm), each at 90 ° to the others. Each of the crystals (0.7 mm diameter) was attached to the long arm of a holder using epoxy resin, and the wires were soldered to a small four-pin connector.

Once implanted, the crystal holders are anchored to the muscle and move as the length of the muscle changes. The sonomicrometer measures a slightly shorter distance than the distance between the holders because the crystals are offset from the holders by a layer of epoxy and because sound emitted from the crystal first traverses a small layer of epoxy through which sound travels faster than it does through muscle. Therefore, it was necessary to calculate an 'offset' to allow a correction from the apparent inter-crystal distance to the actual distance between the connectors (Fig. 1). This correction was carried out by attaching the connectors to a pair of vernier callipers and measuring the offset over a range of inter-connector distances, with the crystals immersed in distilled water contained in a plastic vessel. During calibration, the distance between the crystals was determined using the velocity of sound in water [1498 m s^{-1} at 25 °C (Lide, 1995)].

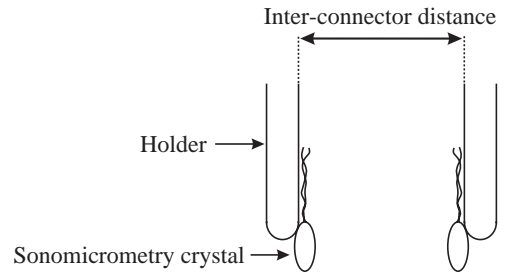


Fig. 1. Illustration of the sonomicrometry crystal holders used to implant the crystals into the pectoralis. The holders are sutured to the muscle fascia to secure the crystals in place. It is the movement of the holders that represents muscle strain, and an offset must therefore be calculated to allow the inter-crystal distance to be converted into strain: $\text{offset} = \text{inter-connector distance} - \text{sonomicrometry distance}$

Electromyography is the main technique used to determine the timing and magnitude of muscle activity (Gans, 1992). An offset hook bipolar electrode was constructed from two twisted strands of Teflon-coated stainless-steel wire (Medwire, AG 3T), with 1.5 mm bared and 3 mm difference in the length between the two tips. Two pairs of electrodes and an additional wire (to ground the bird) were soldered to a small 12-pin connector. The tips of the electrodes were formed into a hook by bending the ends over in a hypodermic needle (the needle was also used to insert the electrodes into the muscle).

Surgical procedure

The sonomicrometry crystals and EMG electrodes were implanted under isoflurane anaesthesia, which was administered at a concentration of 3% to induce and 1.2–2.5% to maintain the anaesthesia. The bird was kept warm (approximately 35 °C) throughout the surgery using a heating pad placed beneath a sterile drape. A strip of feathers was removed from an area overlying the spine and the sternum above the right pectoralis, and the skin was sterilised by swabbing with Betadine. A 10 mm incision was made along the spine, and a 20 mm incision was made above the implantation site of the pectoralis, parallel to the fibres below. Curved surgical scissors were used to tunnel beneath the skin between the two incisions, and a sterile plastic tube (4 mm diameter) was passed through. A pair of sonomicrometry crystals and two pairs of EMG electrodes were passed through the plastic tube to the implantation site, and the tube was then removed. Using a no. 11 scalpel blade, a tiny incision was made parallel to the muscle fascicles and opened to a depth of approximately 2.5 mm with a blunt probe. The sonomicrometry crystal was inserted into this incision and secured in place by suturing the two short arms of the holder to the superficial fascia of the muscle using 6-0 silk. The second crystal was inserted in an identical fashion, approximately 10 mm from the first, along the same fascicle and orientated towards it. Sometimes when the incision was made to insert the holder, the fascicle twitched, facilitating the alignment of the crystals. One pair of EMG electrodes was

inserted on either side of the sonomicrometry recording site and secured using 6-0 silk sutures. Loose wires, including the grounding electrode, were tucked under the skin, and the incisions were closed using 4-0 silk, leaving only the connectors protruding through the skin on the back. The connectors were sutured to the spinal ligaments to keep them in place. Together, they weighed approximately 1.4 g.

In vivo pectoralis strain and EMG activity

A minimum period of 2 h elapsed following surgery for the birds to recover. After this time, they exhibited normal behaviour and readily performed flights. Both take-off and horizontal flights were investigated.

A lightweight 2 m cable (5.6 g), which trailed behind the bird as it flew, was attached between the sonomicrometry system and the connector on the bird's back. Muscle length (L) data were sampled at a frequency of 1050 Hz, using the acquisition software SonoLAB (Sonometrics Corporation, London, Canada) running on a 486DX personal computer. The resting length of the muscle (L_R) was defined as the mean muscle length in the period prior to take-off, corrected for the crystal holder offset (see Fig. 2). Strain was calculated as $(L-L_R)/L_R$. The velocity of sound in muscle was assumed to be 1540 m s^{-1} (Griffiths, 1987). Two smoothing procedures were used on the strain data: a smoothing interpolation using the application IgorPro (WaveMetrics) and smoothing by fitting a Fourier series of the form:

$$L = \frac{a_0}{2} + \sum (a_n \cos nx + b_n \sin nx),$$

where a and b are the Fourier coefficients, n is the harmonic number and x is relative time ($-\pi$ to π). Three harmonics were calculated. Because the wingstrokes were so consistent, there were only slight differences between the two smoothing routines (see Fig. 3A,B).

A second 2 m cable (3.3 g) was attached to the EMG electrodes. Recordings were preamplified using a differential bioamplifier with cut-off filters of 10 Hz and 3000 Hz (DAM50, World Precision Instruments, Sarasota, USA) and sampled using a 12-bit MacAdios II A/D converter at a frequency of 5 kHz. EMG data were synchronized with the strain data using an analog signal obtained from the sonomicrometer and recorded simultaneously with the EMG. This signal only served to synchronize the traces. Analysis of the strain data was performed on the digitally acquired sonomicrometry data.

For the take-off flights, the bird was placed in a covered cardboard cylinder on top of a wire cage in a flight arena constructed from two cardboard screens and mist nets. To induce flight, the lid was removed from the cylinder, and the bird was encouraged from below. The horizontal flights were induced by gently tossing the bird into the air.

After the recordings had been completed, the birds were killed with an intravenous injection of pentobarbital. The pectoralis was exposed, and the positioning of the sonomicrometry crystals along the same fascicle was

confirmed. In all cases, the crystals were found to be well aligned, and no correction was required. The pectoralis and supracoracoideus muscles were dissected from the contralateral side, weighed and the mass doubled to give the total mass of these flight muscles.

In vitro pectoralis power output

The work loop technique (Josephson, 1985) was used to determine the mechanical power output of the pectoralis *in vitro*. Bundles of muscle fascicles were isolated from the pectoralis and subjected to the same length change and activity patterns that had been recorded *in vivo* and to sawtooth cycles with the duration of shortening and lengthening set equal to the *in vivo* values.

To dissect out the pectoralis muscle fibre bundle, the quail was anaesthetised using isoflurane anaesthesia, and the skin overlying the pectoralis was removed. At all times during the dissection, the pectoralis was irrigated using oxygenated Ringer's solution at room temperature (approximately 23°C). The composition of the Ringer's solution (in mmol l^{-1}) was NaCl, 154; glucose, 12; KCl, 6; MgCl_2 , 1; NaH_2PO_4 , 1; MgSO_4 , 1; Hepes, 10; CaCl_2 , 4; pH 7.4 at room temperature, adjusted with the addition of Trizma base. The length of the muscle was measured with the wing maximally elevated, L_{max} . A narrow strip of muscle fascicles was dissected from the superficial region of the pars sternobrachialis of the pectoralis (Dial et al., 1991) running from the central intramuscular tendon to the anterior part of the sternum. Once the muscle had been removed, the bird was killed using an intravenous injection of pentobarbital solution. In a Petri dish containing oxygenated Ringer's solution, the strip of muscle was carefully pared down to approximately 2 mm wide and 1 mm thick. A lightweight connector constructed from links of silver chain and 000 insect pins (mass 51 mg) was tied to the tendon of the muscle using 5-0 silk thread. The muscle was transferred to a chamber through which oxygenated Ringer's solution was circulated using a peristaltic pump (Cole-Parmer, model 7553). The chamber temperature was maintained at $40 \pm 0.01^\circ\text{C}$ by heating a reservoir of Ringer's solution in a water bath (Fisher Scientific). The muscle was secured to the base of the chamber using stainless-steel spring clips, which clamped the sternum on either side of the preparation. The opposite end of the muscle was attached to the arm of an ergometer (Cambridge Technology Inc., series 300B) *via* the lightweight connector. The ergometer was mounted on a stage that could be raised and lowered to vary the length of the muscle. The muscle length was set to $0.9L_{\text{max}}$, which represented the mean resting length of the muscle determined from the *in vivo* sonomicrometry measurements (L_R).

After the dissection, the muscle was left to recover for a brief period (approximately 15 min). After this time, the muscle was stimulated to produce an isometric twitch. A supramaximal stimulus (0.2 ms pulse width) was delivered to the muscle *via* a pair of platinum foil electrodes, which ran down the full length and on either side of the muscle. The stimulus power was amplified using a direct-current power amplifier. This

stimulation regime is designed to activate all the fibres in the bundle simultaneously along their entire length. Twitches were characterised by measuring the latency, twitch-rise time, time from peak force to half-relaxation and time to 90% relaxation. An isometric tetanus was obtained by stimulating the muscle with a 35 ms train of stimuli (frequency 250 Hz).

Work loops were performed by subjecting the muscle to five cyclical contractions. The strain trajectory selected was determined from a typical sonomicrometry recording for a take-off flight. We performed a smoothing interpolation using the application IgorPro (WaveMetrics) to remove the small amount of noise in the sonomicrometry signal. This interpolation also added points so that the resulting wave had 1000 points per cycle. The mean relative timing and duration of the EMGs recorded *in vivo* was used to set the stimulation parameters for the *in vitro* experiments. The ergometer was controlled using a computer-generated wave in the application SuperScope II (version 2.1) and converted into an analog signal by a 16-bit A/D converter. A stimulation wave was synchronised to the length wave and was used to drive a stimulator (Grass), which enabled frequency, train duration and stimulus amplitude to be altered. Force and length outputs were amplified (LPF-202, Warner Instruments, Corp.) and recorded on a Macintosh IICI computer using a 12-bit A/D converter with a sampling frequency of 5 kHz. For comparison with the *in vivo* strain, a sawtooth in which the proportion of the cycle spent shortening was equal to that in the *in vivo* strain trajectory was also studied. The timing and duration of stimulation and the strain amplitude were kept identical to those recorded *in vivo*. For the *in vivo* strain trajectory, strain amplitudes covering most of the range observed during flight were studied (± 10 to $\pm 13\%$). For each series of active cycles, a series of passive cycles was performed, identical in every way to the active cycles but without stimulation. Approximately 3 min was allowed between each set of work loops.

Isometric tetanic contractions were carried out periodically (at least after every five sets of cyclical contractions) to monitor any change in the muscle's performance. Any decline was corrected for by assuming a linear decline in performance between consecutive control tetani.

Results

In vivo flight performance: pectoralis strain and EMG activity

A typical recording of the strain of the pectoralis muscle and EMG activity during take-off is illustrated in Fig. 2. The pectoralis strain trajectory was quite variable during the first few wing strokes (usually the first two or three), tending to be of a lower frequency than during subsequent flaps. The strain trajectory in these later strokes exhibited a highly conserved pattern. Variability towards the end of the flight is due to collision with the mist net. A summary of the muscle strain and timing of EMG activity data for vertical and horizontal flights is presented in Table 1.

Fig. 3C,D shows example pectoralis muscle strain traces from three different birds during both vertical and horizontal flights. Visual comparison of these recordings revealed no differences in the shape of the strain trajectory between the two modes of flight and between individual birds. There were no statistically significant differences in the proportion of the cycle spent shortening, the strain amplitude or the distribution about L_R (Table 1). The strain trajectory of the pectoralis exhibited an asymmetrical temporal pattern, shortening for 70% of the wingstroke. The total strain was $0.23L_R$, with lengthening and shortening approximately equally distributed about L_R . The mean elevation of the wing above L_R was slightly less in level flights than in vertical take-off flights, but this difference was not statistically significant.

Fig. 4A–C shows three typical wing strokes during a vertical take-off flight, and the corresponding muscle shortening velocity. Following the initiation of shortening, the velocity rapidly increased and then briefly decreased. After this brief deceleration, the shortening velocity of the muscle increased throughout most of the remainder of the downstroke, increasing by approximately 80% (e.g. from 5.3 to $9.5 L s^{-1}$ in Fig. 4).

EMG activity was detected during muscle lengthening, 7–8 ms before the muscle reached L_{max} . The duration of activity was 15 ms and so extended into the shortening period of the cycle. There were no statistically significant differences in EMG activity patterns between horizontal and take-off flights (Table 1).

Isometric and morphological properties of quail pectoralis at L_R

The mechanical properties of quail pectoralis are summarised in Table 2, together with the masses of the flight muscles. The pectoralis muscles made up the bulk of the flight

Table 1. Strain and EMG activity measured *in vivo* from quail pectoralis during take-off and horizontal flights

	Vertical take-off flights	Horizontal flights	<i>P</i>
Wingstroke frequency (Hz)	23.2±0.4 (5)	22.6±0.6 (6)	0.32
Proportion of cycle spent shortening (%)	69.6±1.0 (5)	69.1±0.6 (6)	0.67
Peak-to-peak strain (% L_R)	23.4±1.4 (5)	21.4±1.3 (6)	0.45
L_{max} (% greater than L_R)	11.2±2.2 (5)	7.8±2.2 (6)	0.31
EMG duration (ms)	14.8±1.4 (3)	16.4±0.8 (5)	0.32
EMG phase (ms)	-7.8±1.0 (3)	-7.2±0.6 (5)	0.60

Strain characteristics were determined from sonomicrometry recordings.

L_{max} is the muscle length at the maximum wingstroke position reported as the percentage greater than the resting muscle length L_R .

EMG phase represents the timing of EMG onset relative to the maximum wingstroke position for an individual wingstroke.

Values are means \pm S.E.M. (*N*).

The mean values of the two groups have been compared using an unpaired *t*-test. *P* is the probability that the difference between the means is due to random sampling variability.

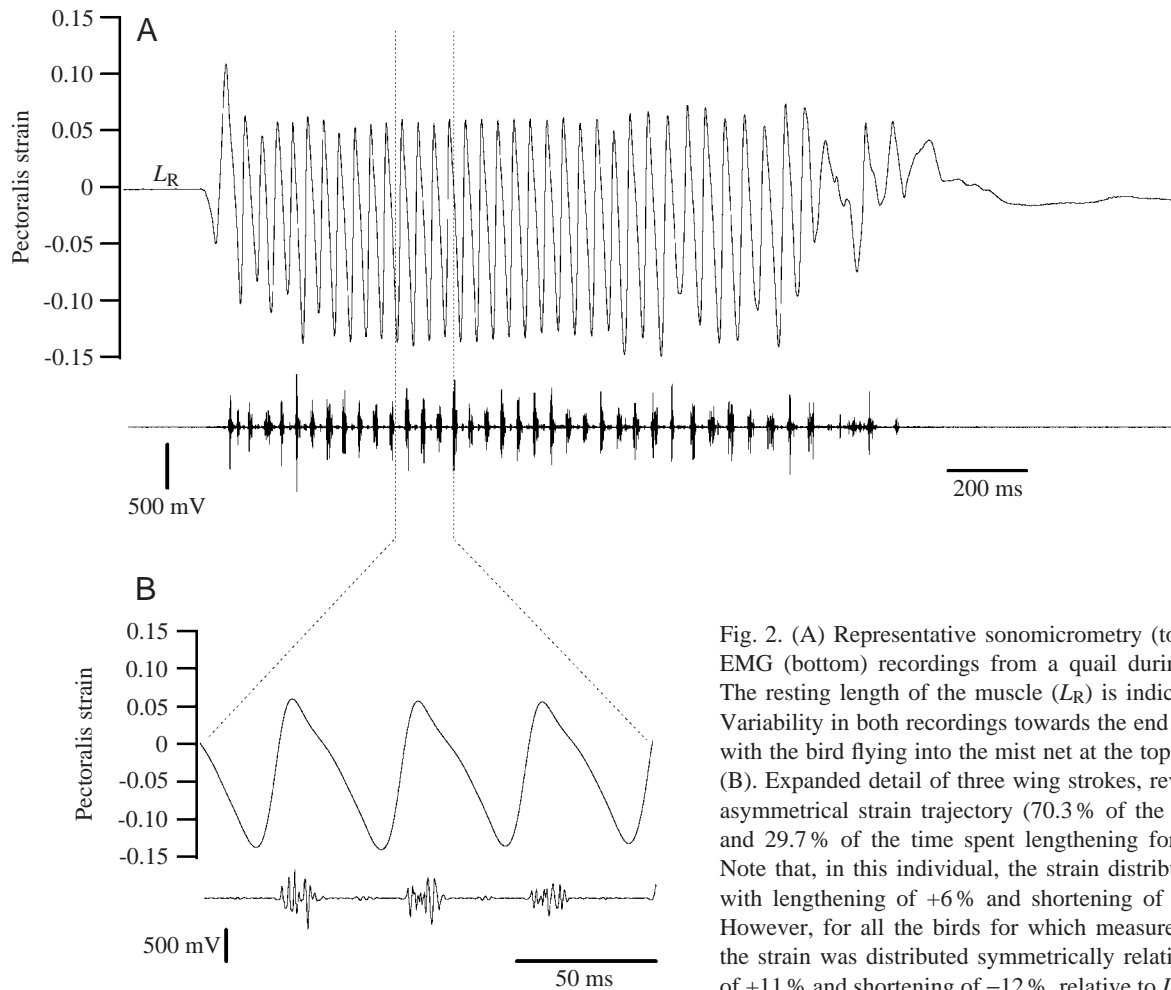


Fig. 2. (A) Representative sonomicrometry (top) and corresponding EMG (bottom) recordings from a quail during a vertical take-off. The resting length of the muscle (L_R) is indicated before the flight. Variability in both recordings towards the end of the flight coincides with the bird flying into the mist net at the top of the flight chamber. (B). Expanded detail of three wing strokes, revealing the temporally asymmetrical strain trajectory (70.3% of the time spent shortening and 29.7% of the time spent lengthening for these three strokes). Note that, in this individual, the strain distribution is asymmetrical, with lengthening of +6% and shortening of -14% relative to L_R . However, for all the birds for which measurements were obtained, the strain was distributed symmetrically relative to L_R (lengthening of +11% and shortening of -12%, relative to L_R ; see Table 1).

muscles, representing 15% of the body mass of the bird. This percentage body mass is similar to reports in the literature for other species in the family Phasianidae: 15% for northern bobwhite, chukar, ring-necked pheasant, wild turkey (Tobalske and Dial, 2000), Japanese quail (Hartman, 1961), 17% for European quail, 18% for black-breasted bobwhite and 22% for grey partridge (Magnan, 1922). The supracoracoideus muscle had a mass of a little over 4% of the body mass. This mass as

a fraction of body mass is much larger than for other species of bird (excluding hummingbirds). The regression equation for a range of flying birds indicates that the supracoracoideus is approximately 1.6% of the body mass (Magnan, 1922; Rayner, 1988). However, larger upstroke muscles are found in birds that have rapid vertical take-offs, typically 5–7% in Phasianidae (Magnan, 1922; Hartman, 1961; Rayner, 1988). In addition, compared with the mass of the pectoralis muscle, the supracoracoideus was relatively larger in quail compared with other birds. Typically, the supracoracoideus is 10% of the mass of the pectoralis muscle (Magnan, 1922), whereas in the blue-breasted quail it was one-third the size of the pectoralis.

The isometric stress at L_R was low (131 kN m^{-2}) in comparison with other measurements at optimal length for vertebrate striated muscle (e.g. 250 kN m^{-2} for mouse limb muscles at a similar temperature; Askew and Marsh, 1997); however, in these experiments on quail, we made no attempt to optimise muscle length (see Discussion).

The latency (the time between the start of EMG activity and the onset of force development) was 3 ms, which was similar to the range of values measured in the sternobranchialis portion of the pectoralis muscle of starlings [3–5 ms (Goslow and Dial, 1990)].

Table 2. *Properties of the quail pectoralis muscle*

Pectoralis mass (% body mass)	15.0 ± 0.6 (10)
Supracoracoideus mass (% body mass)	4.3 ± 0.2 (10)
Isometric stress (kN m^{-2})	130.9 ± 5.4 (8)
Latency (ms)	3.0 ± 0.3 (8)
Twitch rise time (ms)	10.8 ± 0.6 (8)
Twitch half-relaxation time (ms)	8.8 ± 0.3 (8)
Twitch 90% relaxation time (ms)	17.8 ± 0.7 (8)

The contraction kinetics were determined during isometric twitches at resting muscle length, L_R .

The isometric stress is that determined during a 35 ms tetanic contraction at L_R .

Values are means \pm S.E.M. (N).

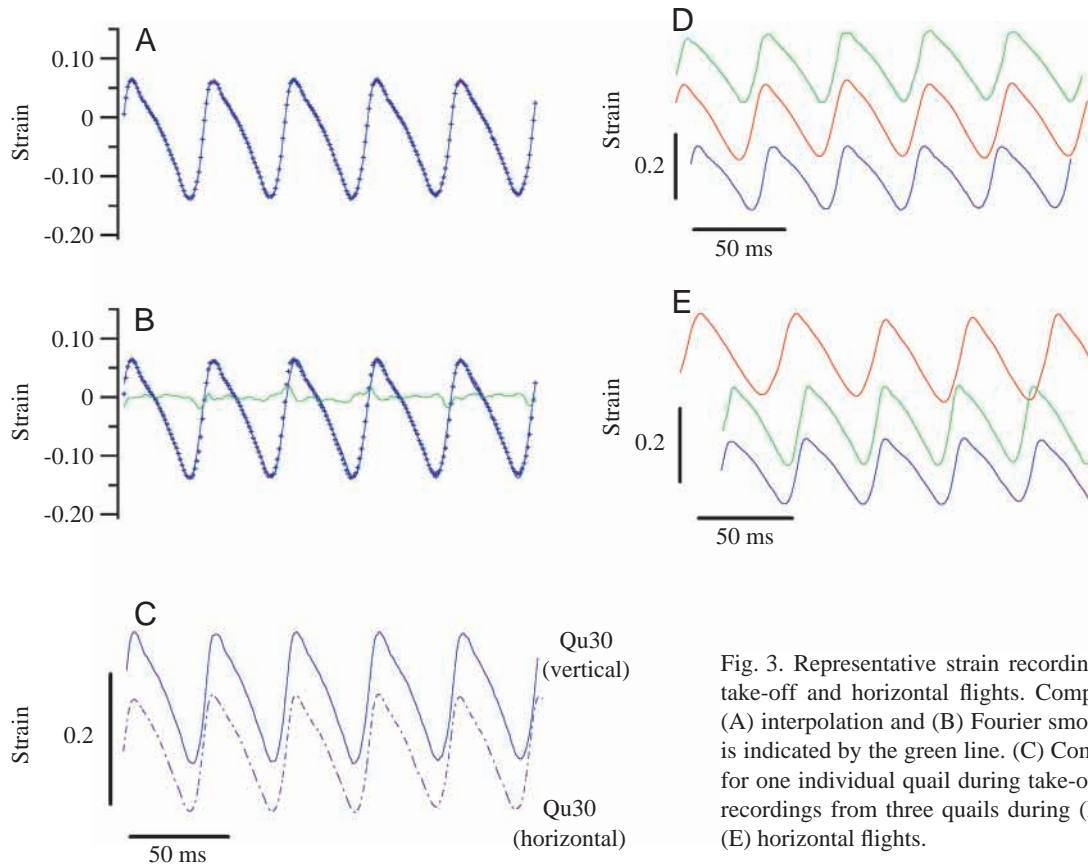


Fig. 3. Representative strain recordings from different quail during take-off and horizontal flights. Comparison of smoothing routines: (A) interpolation and (B) Fourier smoothing. In B, the standard error is indicated by the green line. (C) Comparison of the strain trajectory for one individual quail during take-off and horizontal flights. Strain recordings from three quails during (D) vertical take-off flights and (E) horizontal flights.

In vitro measurement of quail pectoralis power output during work loop contractions

A typical recording from a series of five consecutive wingstrokes from a flight was used as the basis of the wave used to replicate the *in vivo* cycle during *in vitro* work loops (Fig. 5A). An asymmetrical sawtooth wave in which shortening represented 70% of the cycle was also used for comparison (Fig. 5B). The relative timing of stimulation is also indicated for each of the two waveforms by the bold line superimposed on muscle strain.

Fig. 5 summarises the results from a typical *in vitro* experiment, comparing stress (Fig. 5C,D), instantaneous power output (Fig. 5E,F) and the work loops (Fig. 5G,H) for

the two different strain trajectories. The passive force, produced when the muscle was subjected to the strain trajectory without being stimulated, exhibited a large ‘spike’ approximately midway through lengthening, and a similar force was also observed during the active cycles. The magnitude of this force appeared to increase with increasing velocity of stretch, but the relationship was non-linear (Fig. 6). We believe that this force spike during lengthening is an artefact (see Discussion) so, in addition to calculating the net power output, we also calculated the net power generated during shortening averaged over the entire cycle (Table 3). We also measured the peak instantaneous power output and the peak stress during shortening.

Table 3. *Quail pectoralis power output during cyclical contractions in vitro*

	Strain trajectory: Strain amplitude:	Simulation ±11.5%	Simulation ±10%	Simulation ±13%	Sawtooth ±11.5%
Net power output (W kg^{-1})		83.4±39.4 (7)	78.8±57.0 (5)	-110.2±90.9 (5)	67.7±44.2 (8)
Net shortening power averaged over the entire wingstroke (W kg^{-1})		349.1±26.8 (7)	287.0±34.3 (5)	312.3±57.5 (5)	301.9±22.4 (8)
Peak instantaneous power output during shortening (W kg^{-1})		1120.6±122.1 (7)	864.8±81.9 (5)	1227.7±165.4 (5)	1116.2±117.2 (8)
Peak stress during shortening (kN m^{-2})		139.9±22.1 (7)	90.4±15.6 (5)	83.2±13.9 (5)	107.4±14.6 (8)

For each muscle, the power output for each set of experimental conditions was calculated as the average over loops 2–4, inclusive.

The power output presented here is the mean of these data for each strain trajectory.

Strain amplitude is expressed relative to resting muscle length L_R .

The net power output obtained during the natural strain trajectory was approximately 80 W kg^{-1} . However, the power output generated during shortening averaged over the entire wingstroke was 349 W kg^{-1} . The difference between the net power output and the power generated during shortening averaged over the entire cycle was due to the large force spike during lengthening. The same spike was observed for the natural trajectories in which strain amplitude was varied and, in fact, the net power output during the trajectory with a strain amplitude of 13% was negative (Table 3). Because we believe that the force spike was an artefact, and because it is the power generated whilst the pectoralis shortens that contributes to lift and thrust generation, our discussion will concentrate on the power generated during shortening averaged over the wing stroke. The peak instantaneous power output during the *in vivo* length trajectory was 1121 W kg^{-1} (Table 3). The mean power output during shortening was not significantly affected by strain amplitude (Table 3).

Because of the lengthening artefact, we were unable to estimate accurately the work absorbed by the pectoralis muscle due to its activation during the later part of lengthening. This work could be important because *in vivo* it could represent work used to decelerate the wing at the end of the upstroke. On the basis of the moment of inertia calculated from these two values of the wing and the wing's angular velocity (Askew et al., 2001), the maximum work required to decelerate the wing at the end of the upstroke was 3.9 J kg^{-1} . However, in our *in vitro* preparations, the rapid rise in force due to stimulation did not occur until approximately the beginning of shortening, with the peak force occurring well into the shortening phase (Fig. 5, see also Fig. 8).

Work loops, obtained by plotting stress against strain, differed greatly in shape between the two strain trajectories (Fig. 5G,H). During the natural strain cycle, the stress was greatest at the start of shortening, but declined more rapidly than did force during the sawtooth trajectory. The work loops had large components of negative work because of the high force developed during lengthening, which we believe to be an artefact (Fig. 5G,H). This produced large amounts of negative instantaneous power output (Fig. 5E,F) and reduced the net work and power output (Table 3).

Discussion

Condition of the muscle preparation

The muscle preparations were not as robust as those from many ectothermic vertebrates or mammals. Control tetanic contractions indicated that the force typically declined between experimental runs by approximately 6%; however, in the best preparations, the decline was only 0.7% between runs.

Approximately mid-way through lengthening, a large 'force spike' was observed during the cyclical contractions (Fig. 5, Fig. 6). This decreased substantially the net power output of the pectoralis muscle (Table 3). The force spike occurred

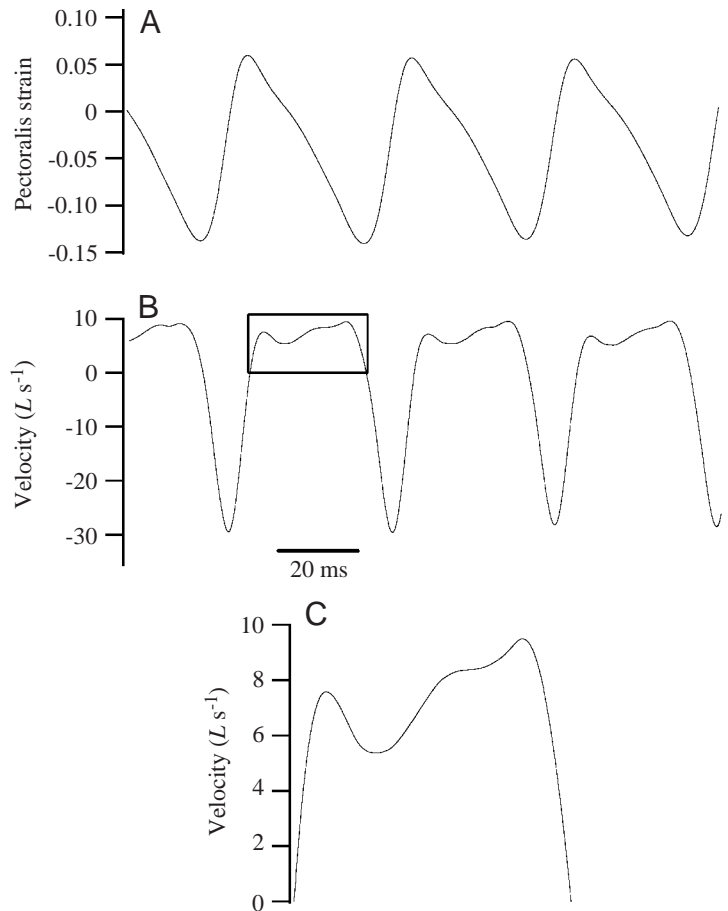


Fig. 4. Variation in muscle shortening velocity over the course of three wingstrokes. (A) Pectoralis strain for typical wingstrokes; (B) the first derivative of strain and (C) details of the velocity during shortening for the cycle marked in B. L , muscle length.

during both active and passive loops, although the phase in the cycle when it occurred was slightly different. We believe that this force during lengthening was an artefact that is unlikely to be found *in vivo*. The force spike does not correspond to the more usual passive elastic force, which is proportional to stretch. Also, its presence in passive muscle indicates that it is not due to previous stimulation and incomplete inactivation.

The origin of this artefact is unclear. One possibility is that it was associated with fibre damage, either along the edges of the preparation, produced during the dissection from the main pectoralis muscle, or with poor oxygenation of the centre of the bundle. However, we would have expected this type of damage to result in slowing of relaxation and high passive force throughout the entire lengthening phase of the cycle. Possibly the artefact is associated with acceleration of the muscle and/or its attachments to the apparatus during lengthening. If the muscle or the silver chain to which it is attached become slack at the shortest length, a force would be required during the lengthening period to accelerate the muscle and its connections to the velocity of the lever at the instant that the slack was taken up. Residual tension in the muscle

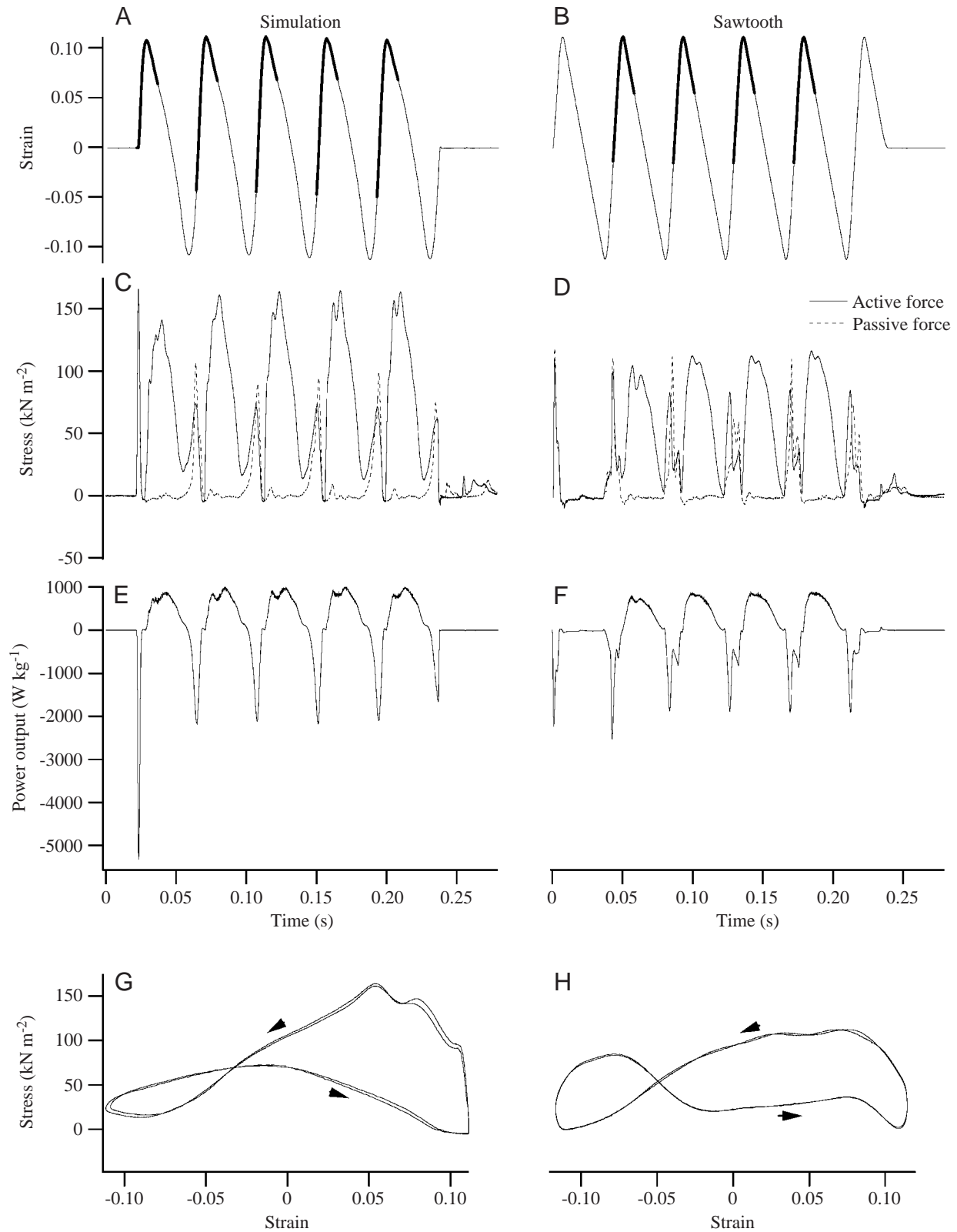


Fig. 5. Examples of data obtained from the *in vitro* work loop experiments. A bundle of muscle fibres was isolated from the quail pectoralis and subjected to a series of cyclical length changes. Two types of strain trajectory were studied: a wave that simulated the strain measured *in vivo* using sonomicrometry (A) and an asymmetrical sawtooth cycle (B). The muscle was activated 7 ms before peak length for 14 ms (indicated by the bold lines in A and B). Force was measured, and this has been used to calculate muscle stress (C,D). The instantaneous power output was calculated by multiplying force by the velocity of shortening (E,F). Work loops were generated by plotting stress against strain. Work loops from two consecutive cycles are shown in G and H. The arrows indicate the direction of the loop.

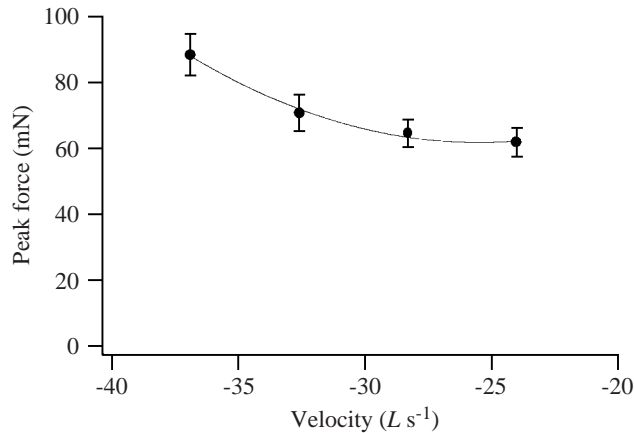


Fig. 6. Peak force during lengthening plotted against the maximum lengthening velocity. Values are means \pm S.E.M. (for at least five muscles). The force during lengthening increased with velocity of stretch, but the relationship was non-linear. The line is a third-order polynomial fitted using least-squares regression. L , muscle length.

during the active cycles might explain the slight phase shift observed between the passive and active cycles. The higher acceleration required with larger strain amplitudes was associated with an increase in the size of the artefact.

Despite the problems encountered with the *in vitro* preparations, we feel that the data collected have considerable value. They represent the first measurements of power output from avian pectoralis muscles *in vitro*. The behaviour of the muscle during shortening appears to be unaffected by the artefact because the force spike is over before shortening begins. Thus, for the purposes of examining the influence of the strain trajectory during shortening, our data are valuable. Because we believe that this force spike during lengthening is an artefact, we calculated both the net power and the net power generated during shortening averaged over the entire cycle (Table 3). This latter measure of the pectoralis power output is the relevant value for comparing with the power we measured during climbing flights (Askew et al., 2001). Any work done on the pectoralis during the upstroke would have to be supplied by the supracoracoideus and any other upstroke muscles. This internal use of energy would not show up in calculations based on flight kinematics. The remainder of the discussion will concentrate on the physiological behaviour of the muscle during shortening.

Isometric properties

The isometric stress measured at L_R was lower than the peak isometric stress (P_0) typically reported for vertebrate skeletal muscle [e.g. 243 kN m^{-2} for mouse soleus muscle (Askew and Marsh, 1997); 188 kN m^{-2} for lizard muscle (Marsh and Bennett, 1986)] and lower than that reported (Johnston, 1985) for quail pectoralis muscle (200 kN m^{-2}). In most estimations of isometric stress *in vitro*, the length of the muscle is optimised (the optimal length usually being termed L_0) during a series of tetani to maximise the force developed. However, in these experiments, we were interested in reproducing as

closely as possible the muscle's functioning *in vivo*, so we did not optimise muscle length. The length at which we measured the isometric stress was the resting length of the muscle (L_R), defined *in vivo* as the length of the pectoralis muscle in the period prior to take-off. The peak stress occurred early in the shortening phase of the length trajectory (Fig. 5C,D) and then declined throughout the remainder of muscle shortening (Table 3). The peak stress measured during the natural work loops actually exceeded by 7% the isometric stress measured at L_R . In other optimised work loops oscillating symmetrically about L_0 , the peak stress is usually approximately $0.4P_0$, at the cycle frequency that gives the maximum power output (Askew and Marsh, 1998). These observations suggest that the optimum length for force generation was higher than L_R . In support of this argument, much higher stresses comparable with those in other vertebrate muscles were obtained by increasing the length to L_{max} ; however, a systematic investigation was not carried out.

A muscle is alternately activated and deactivated during a cyclical contraction. To maximize work, the muscle must be activated so that it develops force during shortening and deactivated to maintain minimal force during lengthening. The twitch rise time is a measure of the rate of deactivation of the muscle, since force only starts to decline once there is a net detachment of crossbridges due to sequestration of Ca^{2+} (Marsh, 1990). To allow comparison of our twitch parameters with those for other muscles in the literature, we plotted the time available for shortening (taken as half the cycle duration in the absence of *in vivo* data) against twitch rise time. A strong correlation was observed ($r^2=0.935$; $P<0.01$; Fig. 7), and the twitch rise time for quail was found to be comparable with that of other muscles used at a similar cycle frequency, such as the calling muscles of hylid tree frogs (McLister et al., 1995; Girgenrath and Marsh, 1999), zebra finch pectoralis muscle (Hagiwara et al., 1968) and a locust flight muscle (Josephson and Stevenson, 1991).

In vivo strain trajectory

Our sonomicrometry recordings confirmed our hypothesis that the pectoralis muscle would exhibit an asymmetrical strain trajectory. The *in vivo* length trajectory was highly conserved between individual birds and during both take-off and horizontal flights. During take-off, 70% of the cycle was spent shortening (Fig. 2; Table 1). The relative duration of the downstroke is longer than has been measured directly in pigeons in level flight [63% (Biewener et al., 1998)] and other Phasianidae [56% in wild turkey; 64% in northern bobwhite (Tobalske and Dial, 2000)] and equal to that estimated from kinematics during take-off in Rüppell's griffon vulture (Scholey, 1983).

Asymmetrical contractile cycles have been observed in the external oblique muscles involved during calling in hylid tree frogs (Girgenrath and Marsh, 1997). It has been shown that muscles performing asymmetrical cycles with a longer duration of shortening generate a higher net power output than those performing symmetrical cycles. For example, the tree frog calling muscles generated 60% more power during

asymmetrical sawtooth cycles with 75% shortening (saw75%) than during sinusoidal cycles (Girgenrath and Marsh, 1999). Mouse skeletal muscles performing saw75% cycles generated 38% more power compared with saw50% cycles and 50% more power compared with sinusoidal cycles (Askew and Marsh, 1997). There are several reasons why the net power output is increased as the proportion of the cycle spent shortening increases. First, the muscle becomes more completely activated as there is more time available for force development. Also, more time is available for relaxation during shortening, which ensures that the residual force during lengthening is low and that the work required to re-extend the muscle is minimal. The optimal strain amplitude increases and, finally, the rate of development of force increases with the velocity of stretch, which increases the work generated during the subsequent shortening period (Askew and Marsh, 1997; Askew and Marsh, 1998). Increasing the relative shortening duration is an alternative to increasing the maximum shortening velocity of the muscle and is particularly important in muscles that operate at high cycle frequencies (Askew and Marsh, 1997).

In vitro assessment of power output using the work loop technique

The power output produced *in vitro* at 23 Hz during simulated flight contractions by quail pectoralis is high. The net power measured during shortening, but averaged over the whole cycle, was approximately 350 W kg^{-1} , with a maximum recorded of 433 W kg^{-1} . This compares with net power outputs from other fast vertebrate muscles of 150 W kg^{-1} at 20 Hz for in the iliofibularis of the lizard *Dipsosaurus dorsalis* (Swoap et al., 1993) and 200 W kg^{-1} in mouse extensor digitorum longus (EDL) at 9 Hz during sawtooth cycles with 75% of the time spent shortening, a strain trajectory resembling that found naturally in the quail pectoralis muscle (Askew and Marsh, 1997). We suspect that the unusual performance of the quail pectoralis relies on unusual intrinsic properties and, in addition, on the detailed shape of its strain trajectory during shortening.

In past studies, the maximum power output obtained from force/velocity curves is higher, usually approximately threefold, than during cyclical contractions. For example, the

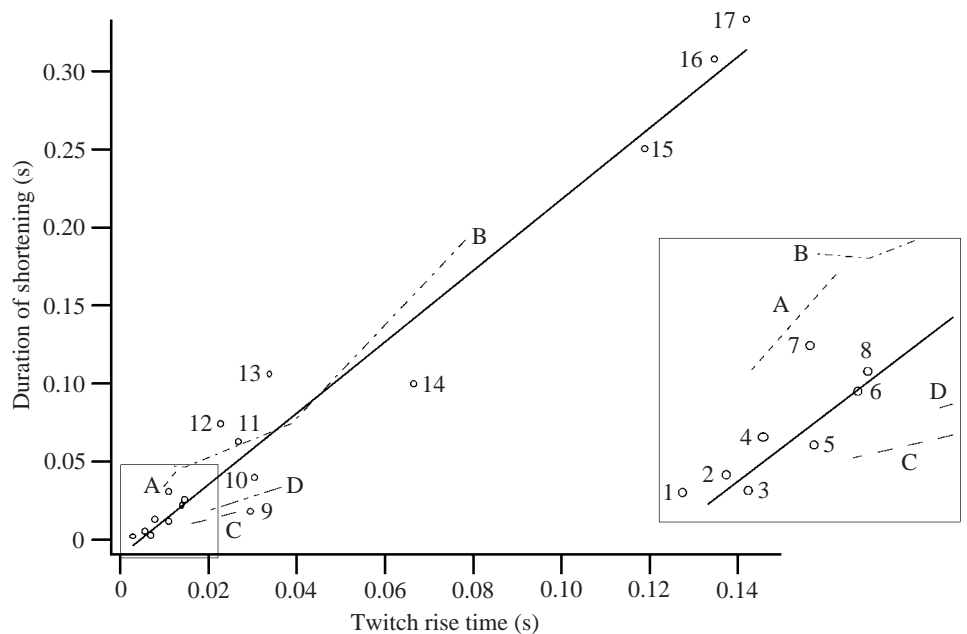


Fig. 7. Relationship between shortening duration and twitch rise time for a variety of muscles: (1) cicada singing muscle (Josephson, 1984), (2) rattlesnake shaker muscle (Rome et al., 1996), (3) toadfish swimbladder muscle (Rome et al., 1996), (4) hummingbird pectoralis muscle (Hagiwara et al., 1968), (5) *Hyla chrysoscelis* external oblique muscle (Girgenrath and Marsh, 1999), (6) zebra finch pectoralis muscle (Hagiwara et al., 1968), (7) blue-breasted quail pectoralis muscle (this study), (8) locust flight muscle (Josephson and Stevenson, 1991), (9) *Hyla versicolor* external oblique muscle (Girgenrath and Marsh, 1999), (10) starling pectoralis muscle (Goslow and Dial, 1990), (11) saithe white muscle at 0.35 body lengths from the anterior tip (Altringham et al., 1993), (12) scup pink muscle at 20 °C (Coughlin et al., 1996), (13) scup red muscle (Swank et al., 1997), (14) toadfish white muscle (Rome et al., 1996), (15) rainbow trout slow muscle at 0.35 body lengths from the rostral tip (Hammond et al., 1998), (16) *Argopecten irradians* adductor muscle (Olson and Marsh, 1993), (17) toadfish red muscle (Rome et al., 1996). The lines represent data from several different temperatures: (A) *Dipsosaurus dorsalis* iliofibularis muscle (Marsh, 1988), (B) *Dipsosaurus dorsalis* iliofibularis muscle (Swoap et al., 1993), (C) *Hyla chrysoscelis* tensor chordarum muscle (McLister et al., 1995), (D) *Hyla versicolor* tensor chordarum muscle (McLister et al., 1995). The solid, bold line represents the linear regression for all the data ($r^2=0.935$, $P<0.01$). For most of the muscles, the twitch rise time was the time from zero to maximum force; however, for the scup pink muscle, it was the time taken from 10% to 90% of the peak force.

peak isotonic power for the iliofibularis of *Dipsosaurus dorsalis* is 460 W kg^{-1} [at 40 °C (Marsh and Bennett, 1985)] and for the mouse EDL it is 370 W kg^{-1} (Askew and Marsh, 1997). Given the high power output of quail muscle at 23 Hz, one might expect this muscle to have a particularly high maximum velocity of shortening V_{\max} . Preliminary measurements during afterloaded isotonic contractions indicate a V_{\max} of 32 L s^{-1} for this muscle (G. N. Askew and R. L. Marsh, unpublished observations).

In addition to the obvious temporal asymmetry, the performance of the quail pectoralis also benefits from more subtle aspects of the strain trajectory. Of the two strain trajectories used in the *in vitro* experiments, both had the same average shortening velocity (the strain amplitude and the duration of shortening are the same), but they differed in the velocity distribution (Fig. 8). In the sawtooth cycle, the shortening velocity was held constant, whereas the shortening

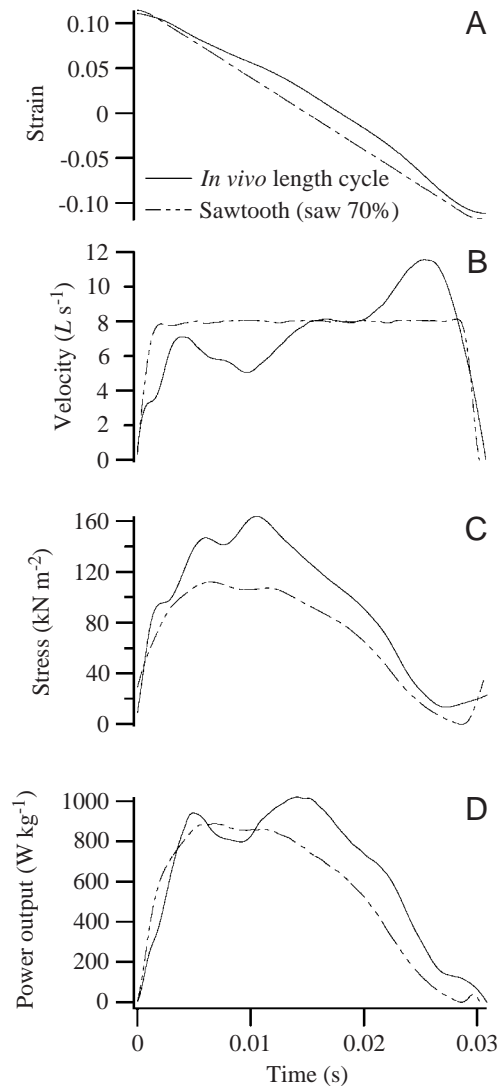


Fig. 8. Comparison of the strain (A) and shortening velocity (B) during shortening for the simulation and sawtooth cycles and the stress (C) and instantaneous power output (D) that is developed. The stress was higher during the simulation cycle than during the sawtooth cycle throughout most of shortening, but the instantaneous power output was only greater during the later part of shortening. L , muscle length.

velocity increased during shortening in the simulation cycle (Fig. 4, Fig. 8B). During shortening, this was the only difference between the two cycles. On the basis of the predictions of the force/velocity relationship, the sawtooth cycle with constant shortening velocity should have yielded a higher net power output; however, the average power output during shortening was 16% greater during the simulation cycle than during the sawtooth trajectory (Table 3; not statistically significant $P < 0.2$).

In Fig. 8, strain, velocity, stress and instantaneous power output are shown for the shortening phase of a typical cycle. The main difference is that the stress is greater throughout almost the entire shortening period in the simulation cycle. The

discrepancy is greatest at the start of shortening, when the velocity during the *in vivo* length cycle is low, resulting in high forces (presumably due to force/velocity effects). However, in the first third of the shortening period, there is essentially no difference in the instantaneous power output delivered during either strain trajectory (because the high forces obtained during the simulation cycle also correspond to a low shortening velocity). The main difference in power distribution occurs over the second half of the shortening period, with the greatest discrepancy occurring approximately mid-way through shortening. This is perhaps surprising because the shortening velocity is approximately equal in both strain trajectories at this point. However, we think that this results from the higher lengthening velocity during the simulation strain trajectory. During lengthening, the peak velocity is $33 L s^{-1}$ for the simulation cycle and $24 L s^{-1}$ during the sawtooth cycle. Stretching a muscle early in the activation period results in it developing force more rapidly (Hill, 1970). The rate of force development increases with increasing velocity of stretch, perhaps as a result of an increase in net crossbridge attachment (Askew and Marsh, 1998). Therefore, the higher velocity of stretch during the simulation compared with the sawtooth cycle may result in a higher rate of activation of the pectoralis, which enables the force to be higher midway through shortening during the simulation cycle despite the shortening velocity being equal. During the latter part of shortening, the rate of deactivation of force is greater in the simulation than in the sawtooth cycle (Fig. 8C). This rapid deactivation occurs at the point in the cycle at which the shortening velocity is highest and is 50% greater than in the sawtooth cycles. This is consistent with the velocity-dependent deactivation observed in other muscles, where the rate of deactivation of a relaxing muscle increases with increasing shortening velocity (Askew and Marsh, 1998). This depression of force is in addition to force/velocity effects and appears to be due to the release of extra Ca^{2+} from troponin, which occurs in proportion to the rate of shortening (Gordon and Ridgway, 1987; Caputo et al., 1994). Rapid deactivation at the end of shortening ensures that there is little residual force during re-lengthening of the pectoralis on the upstroke, which would increase the power required from the supracoracoideus. However, even during this relaxation period, the instantaneous power output is greater during the simulation trajectory than during the sawtooth trajectory, because of the higher stress and higher shortening velocity.

Strain amplitude and shortening velocity

The total muscle strain was relatively large (23%; Fig. 2; Table 1), as has been found in other avian flight muscles. For example, strains of 32% in pigeon pectoralis muscle (Biewener et al., 1998) and of 29% during level flight and 36% during ascending flight in mallard pectoralis muscle (Williamson et al., 2001) have been measured using sonomicrometry. In the Phasianidae, pectoralis muscle strain during take-off is approximately 22% in birds ranging in size from 0.04 to 1 kg. Measured strains are higher in the 5.3 kg

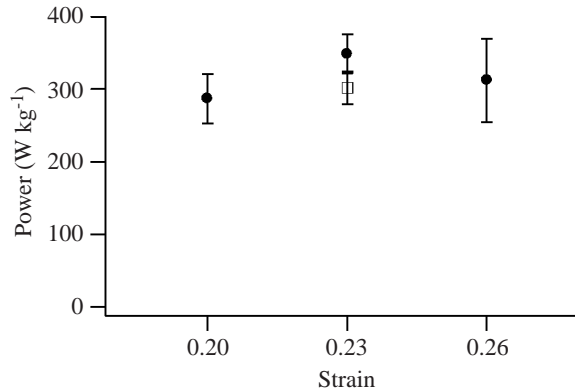


Fig. 9. Variation in the mean power during shortening averaged over the entire cycle period with total strain for the simulation length-change cycles. For comparison, data for the sawtooth cycle have also been included (open square); however for these cycles, strain was not varied. Values are means \pm S.E.M., $N=5-8$.

turkey (35%), but the overall scaling relationship is not significant (Askew et al., 2001). Other *in vivo* muscle strain measurements range from 1.9% in bumblebee flight muscle (Gilmour and Ellington, 1993) to 7–12% in the calling muscles of hylid tree frogs (Girgenrath and Marsh, 1997) and 22.5% in scallop adductor muscle (Olson and Marsh, 1993; Marsh and Olson, 1994). The strain observed *in vivo* was found to be optimal for generating maximum net power output *in vitro* compared with strains 3% lower and 3% higher than L_R (Fig. 9). The calling muscles of hylid tree frogs and the adductor muscle in swimming scallops have also been found to operate *in vivo* strains that maximise power *in vitro* (Girgenrath and Marsh, 1997; Girgenrath and Marsh, 1999; Marsh and Olson, 1994).

The high strain amplitude measured for the quail pectoralis muscle corresponds to an average shortening velocity of $7.8 L s^{-1}$. On the basis of preliminary estimates of V_{max} from isovelocity shortening contractions, this corresponds to a V/V_{max} of 0.24 ($V_{max}=32 L s^{-1}$, G. N. Askew and R. L. Marsh, unpublished observations). The peak isotonic power output occurs at a much higher velocity, $0.37 V_{max}$. The force/velocity relationship has frequently been used to predict the shortening velocity at which muscles are expected to operate [e.g. Rome (Rome, 1994)]; however, our experiments on mouse skeletal muscles showed that this simple prediction does not hold for cyclical contractions under varied conditions (Askew and Marsh, 1998). The optimal relative shortening velocity for generating maximal power output depends on the force/velocity characteristics of the muscle, the length/force relationship and the rate of activation and deactivation. In cycles in which the strain amplitude is high, for example during strain trajectories in which the proportion of time spent shortening is greater than that spent lengthening, the length/force relationship reduced the optimal V/V_{max} below that predicted from the force/velocity curve. The strain of quail pectoralis is large (23% L_R), and force will be reduced by the length/force relationship. However, the effects of the

length/force relationship are further increased because the optimum length of the muscle is greater than the resting length (L_R) and appears to be close to L_{max} .

Significance for *in vivo* muscle performance

The question arises as to how the values measured *in vitro* in bundles of fibres should be interpreted in terms of the capacity for whole-muscle power output during flight (Askew et al., 2001). The complexities of most locomotor systems have prevented direct comparisons of the performance of individual muscles *in vivo* and *in vitro*. However, using the simple locomotor system of the scallop, previous studies have demonstrated that, given accurate data on the length trajectory and stimulation regime, an *in vitro* preparation can accurately reproduce the details of power output as measured *in vivo* (Marsh et al., 1992; Marsh and Olson, 1994). Of course, such comparisons always rely on obtaining and maintaining undegraded *in vitro* preparations. In the present study, we based our *in vitro* work on the strain trajectory measured at only one location. Biewener et al. (Biewener et al., 1998) demonstrated regional differences in strain in the pigeon pectoralis, but the effect of these differences on power output is not known because they have no data on regional differences in stress. Stress and strain are reciprocally linked *via* force/velocity effects. In our preparations, varying strain from 0.2 to 0.26 had no significant effect on power output. In terms of stimulation regime, our *in vitro* preparations are fully stimulated and should accurately reflect the power output of the active fraction of the muscle *in vivo*. Such a stimulation regime will overestimate the *in vivo* power if *in vivo* recruitment is not maximal. Despite the complexities of the comparisons, we believe that the *in vivo* and *in vitro* measurements are valuable as independent measures of the capacity of the flight muscles. The *in vitro* approach has particular value in being able to test the importance of particular features of the *in vivo* cycle, as was done here with the strain trajectory during shortening.

Concluding remarks

We found that the mean power output of the pectoralis muscle during shortening averaged over the entire cycle from blue-breasted quail *Coturnix chinensis* during *in vitro* simulations of the *in vivo* length and activity patterns was $350 W kg^{-1}$ (average of all muscles) and as high as $433 W kg^{-1}$ (maximum). This compared with an average power output of $390 W kg^{-1}$ and a maximum for one individual of $530 W kg^{-1}$ estimated from the movement of the centre of mass and the aerodynamic requirements (Askew et al., 2001). This is the highest power output yet measured *in vitro* and was achieved with the asymmetrical length cycle (relative downstroke duration 70%) and subtle changes in shortening velocity during the shortening period.

This work was supported by a Wellcome Research Travel Grant (to G.N.A.) and by the NIH (grant AR39318 to R.L.M.).

References

- Altringham, J. D., Wardle, C. S. and Smith, C. I. (1993). Myotomal muscle function at different locations in the body of a swimming fish. *J. Exp. Biol.* **182**, 191–206.
- Askew, G. N. and Marsh, R. L. (1997). The effects of length trajectory on the mechanical power output of mouse skeletal muscles. *J. Exp. Biol.* **200**, 3119–3131.
- Askew, G. N. and Marsh, R. L. (1998). Optimal shortening velocity (V/V_{\max}) of skeletal muscle during cyclical contractions: length–force effects and velocity-dependent activation and deactivation. *J. Exp. Biol.* **201**, 1527–1540.
- Askew, G. N., Marsh, R. L. and Ellington, C. P. (2001). The mechanical power output of the flight muscles of blue-breasted quail (*Coturnix chinensis*) during take-off. *J. Exp. Biol.* **204**, 3601–3619.
- Biewener, A. A., Corning, W. R. and Tobalske, B. W. (1998). *In vivo* pectoralis muscle force–length behavior during level flight in pigeons (*Columba livia*). *J. Exp. Biol.* **201**, 3293–3307.
- Biewener, A. A., Dial, K. P. and Goslow, G. E. (1992). Pectoralis muscle force and power output during flight in the starling. *J. Exp. Biol.* **164**, 1–18.
- Caputo, C., Edman, K. A. P., Lou, F. and Sun, Y.-B. (1994). Variation in myoplasmic Ca^{2+} concentration during contraction and relaxation studied by the indicator fluo-3 in frog muscle fibres. *J. Physiol., Lond.* **478**, 137–148.
- Coughlin, D. J., Zhang, G. and Rome, L. C. (1996). Contraction dynamics and power production of pink muscle of the scup (*Stenotomus chrysops*). *J. Exp. Biol.* **199**, 2703–2712.
- Dial, K. P. and Biewener, A. A. (1993). Pectoralis muscle force and power output during different modes of flight in pigeons (*Columba livia*). *J. Exp. Biol.* **176**, 31–54.
- Dial, K. P., Biewener, A. A., Tobalske, B. W. and Warrick, D. R. (1997). Mechanical power output of bird flight. *Nature* **390**, 67–70.
- Dial, K. P., Goslow, G. E. and Jenkins, F. A., Jr (1991). The functional anatomy of the shoulder in the European starling (*Sturnus vulgaris*). *J. Morph.* **207**, 327–344.
- Dial, K. P., Kaplan, G. E., Goslow, G. E., Jr and Jenkins, F. A., Jr (1988). A functional analysis of the primary upstroke and downstroke muscles in the domestic pigeon (*Columba livia*) during flight. *J. Exp. Biol.* **134**, 1–16.
- Gans, C. (1992). Electromyography. In *Biomechanics: Structures and Systems* (ed. A. A. Biewener), pp. 175–204. Oxford: Oxford University Press.
- Gilmour, K. M. and Ellington, C. P. (1993). *In vivo* length changes inbumblebees and the *in vitro* effects on work and power. *J. Exp. Biol.* **183**, 101–113.
- Girgenrath, M. and Marsh, R. L. (1997). *In vivo* performance of trunk muscles in tree frogs during calling. *J. Exp. Biol.* **200**, 3101–3108.
- Girgenrath, M. and Marsh, R. L. (1999). Power of sound-producing muscles in the gray tree frogs *Hyla versicolor* and *Hyla chrysoscelis*. *J. Exp. Biol.* **202**, 3225–3237.
- Gordon, A. M. and Ridgway, E. B. (1987). Extra calcium on shortening in barnacle muscle: Is the decrease in calcium binding related to decreased crossbridge attachment, force or length? *J. Gen. Physiol.* **90**, 321–340.
- Goslow, G. E. and Dial, K. P. (1990). Active stretch–shorten contractions of the m. pectoralis in the European starling (*Sturnus vulgaris*): evidence from electromyography and contractile properties. *Neth. J. Zool.* **40**, 106–114.
- Griffiths, R. I. (1987). Ultrasound transit time gives direct measurement of muscle fibre length *in vivo*. *J. Neurosci. Meth.* **21**, 159–165.
- Hagiwara, S., Chichibu, S. and Simpson, N. (1968). Neuromuscular mechanisms of wing beat in hummingbirds. *Z. Vergl. Physiol.* **60**, 209–218.
- Hammond, L., Altringham, J. D. and Wardle, C. S. (1998). Myotomal muscle function of rainbow trout *Oncorhynchus mykiss* during steady swimming. *J. Exp. Biol.* **201**, 1659–1671.
- Hartman, F. A. (1961). Locomotor mechanisms of birds. *Smithsonian Misc. Collns.* **143**, 1–91.
- Hill, A. V. (1970). *First and Last Experiments in Muscle Mechanics*. Cambridge: Cambridge University Press.
- Johnston, I. A. (1985). Sustained force development: specializations and variation among the vertebrates. *J. Exp. Biol.* **115**, 239–251.
- Josephson, R. K. (1984). Contraction dynamics of flight and stridulatory muscles of tettigoniid insects. *J. Exp. Biol.* **108**, 77–96.
- Josephson, R. K. (1985). Mechanical power output from striated muscle during cyclical contractions. *J. Exp. Biol.* **114**, 493–512.
- Josephson, R. K. and Stevenson, R. D. (1991). The efficiency of a flight muscle from the locust *Schistocerca americana*. *J. Physiol., Lond.* **442**, 413–429.
- Lide, D. R. (1995). *CRC Handbook of Chemistry and Physics (1913–1995)*. 75th edition. London: CRC Press Inc.
- Magnan, A. (1922). Les caractéristiques des oiseaux suivant le mode de vol. *Ann. Sci. Nat. Dixième Série* **5**, 125–334.
- Marsh, R. L. (1988). Ontogenesis of contractile properties of skeletal muscle and sprint performance in the lizard *Dipsosaurus dorsalis*. *J. Exp. Biol.* **137**, 119–139.
- Marsh, R. L. (1990). Deactivation rate and shortening velocity as determinants of contractile frequency. *Am. J. Physiol.* **259**, R223–R230.
- Marsh, R. L. (1999). How muscles deal with real-world loads: the influence of length trajectory on muscle performance. *J. Exp. Biol.* **202**, 3377–3385.
- Marsh, R. L. and Bennett, A. F. (1985). Thermal dependence of isotonic contractile properties of skeletal muscle and sprint performance of the lizard *Dipsosaurus dorsalis*. *J. Comp. Physiol. B* **155**, 541–551.
- Marsh, R. L. and Bennett, A. F. (1986). Thermal dependence of contractile properties of skeletal muscle from the lizard *Sceloporus occidentalis* with comments on methods for fitting and comparing force/velocity curves. *J. Exp. Biol.* **126**, 63–77.
- Marsh, R. L. and Olson, J. M. (1994). Power output of scallop adductor muscle during contractions replicating the *in vivo* mechanical cycle. *J. Exp. Biol.* **193**, 139–156.
- Marsh, R. L., Olson, J. M. and Guzik, S. K. (1992). Mechanical performance of scallop adductor muscles during swimming. *Nature* **357**, 411–413.
- McLister, J. D., Stevens, E. D. and Bogart, J. P. (1995). Comparative contractile dynamics of calling and locomotor muscles in three hylid tree frogs. *J. Exp. Biol.* **198**, 1527–1538.
- Norberg, U. M. (1990). *Vertebrate Flight: Mechanics, Physiology, Morphology, Ecology and Evolution*. Berlin: Springer-Verlag.
- Olson, J. M. and Marsh, R. L. (1993). Contractile properties of the striated adductor muscle in the bay scallop *Argopecten irradians* at several temperatures. *J. Exp. Biol.* **176**, 175–193.
- Rayner, J. M. V. (1988). Form and function in avian flight. In *Current Ornithology* vol. 5, chapter 1 (ed. R. F. Johnston), pp. 1–66. New York: Plenum Press.
- Rayner, J. M. V. (1993). On aerodynamics and energetics of vertebrate flapping flight. *Contemp. Math.* **141**, 351–400.
- Rome, L. C. (1994). The mechanical design of the muscular system. In *The Advances in Veterinary Science and Comparative Medicine: Comparative Vertebrate Exercise Physiology* (ed. J. H. Jones), pp. 125–179. New York: Academic Press.
- Rome, L. C., Syme, D. A., Hollingworth, S., Lindstedt, S. L. and Baylor, S. M. (1996). The whistle and the rattle: the design of sound producing muscles. *Proc. Natl. Acad. Sci. USA* **93**, 8095–8100.
- Scholey, K. D. (1983). Developments in vertebrate flight: climbing and gliding in mammals and reptiles and the flapping flight of birds. PhD thesis, University of Bristol.
- Swank, D. M., Zhang, G. and Rome, L. C. (1997). Contraction kinetics of red muscle in scup: mechanism for variation in relaxation rate along the length of the fish. *J. Exp. Biol.* **200**, 1297–1307.
- Swoap, S. J., Johnson, T. P., Josephson, R. K. and Bennett, A. F. (1993). Temperature, muscle power output and limitations on burst performance of the lizard *Dipsosaurus dorsalis*. *J. Exp. Biol.* **174**, 185–197.
- Tobalske, B. W. and Dial, K. P. (2000). Effects of body size on take-off flight performance in the Phasianidae (Aves). *J. Exp. Biol.* **203**, 3319–3332.
- Westneat, M. W. (1996). Functional morphology of aquatic flight in fishes: kinematics, electromyography and mechanical modeling of labriform locomotion. *Am. Zool.* **36**, 582–598.
- Williamson, M. R., Dial, K. P. and Biewener, A. A. (2001). Pectoralis muscle performance during ascending and slow level flight in mallards (*Anas platyrhynchos*). *J. Exp. Biol.* **204**, 495–507.
- Willmott, A. P. and Ellington, C. P. (1997). The mechanics of flight in the hawkmoth *Manduca sexta*. I. Kinematics of hovering and forward flight. *J. Exp. Biol.* **200**, 2705–2722.